Inorg. Chem. **2007**, *46*, 2814–2823

Synthesis and Characterization of the Homoleptic Octahydrotriborate Complex $Cr(B_3H_8)_2$ and Its Lewis Base Adducts

Dean M. Goedde, G. Kenneth Windler, and Gregory S. Girolami*

School of Chemical Sciences, University of Illinois at Urbana—Champaign, 600 South Mathews Avenue, Urbana, Illinois 61801

Received November 10, 2006

Solvate-free sodium octahydrotriborate, NaB_3H_8, is prepared on a 20 gram scale from sodium amalgam and diborane in diethyl ether. This substance, which is chemically related to borohydride-based compounds being investigated as hydrogen storage materials, is also useful for the preparation of transition-metal complexes bearing B_3H_8 ligands. Treatment of $CrCl_3$ with NaB_3H_8 affords a thermally unstable purple liquid thought to be a chromium(III) hydride of stoichiometry $CrH(B_3H_8)_2$. This hydride converts rapidly at room temperature to the chromium(II) complex $Cr(B_3H_8)_2$, which adopts a square-planar structure in which four hydrogen atoms form the coordination sphere of the chromium atom. This chromium(II) species forms six-coordinate Lewis base adducts $Cr(B_3H_8)_2L_2$, where L is Et_2O, THF, or PMe_3; the first two of these adopt trans geometries, whereas the latter is cis. Volatile $Cr(B_3H_8)_2$ is the first homoleptic transition-metal complex of the octahydrotriborate anion, and it is an excellent single-source precursor for the chemical vapor deposition of thin films of CrB_2 at temperatures as low as 200 °C. Crystal structures of the new complexes are reported.

Introduction

Molecular complexes that contain only metal, boron, and hydrogen are of interest, owing to their catalytic properties,[1] their utility as CVD precursors,[2−8] and their usefulness as starting materials for other inorganic species.[9,10] The pyrophoric nature of most metal tetrahydroborate complexes has even been exploited in a patent for a cigarette lighter that employs $Al(BH_4)_3$ as the ignition source.[11] Of the 11 known molecular complexes of stoichiometry MB_xH_y, all but one possess BH_4 ligands; these are the homoleptic metal tetrahydroborate complexes of Be^{II},[12] Al^{III},[13,14] Ti^{III},[15,16] Zr^{IV},[17−19] Hf^{IV},[17,20] Th^{IV},[17] Pa^{IV},[21,22] U^{IV},[15,23−25] Np^{IV},[21,22,25] and Pu^{IV}.[21,22] Of these, the binary BH_4 complexes of Be, Al, Ti, Zr, Hf,

* To whom correspondence should be addressed. E-mail: girolami@scs.uiuc.edu.

(1) Panchenko, V. N.; Zakharov, V. A.; Echevskaya, L. G.; Nesterov, G. A. *Vysokomol. Soedin., Ser. A Ser. B* **1994**, *36*, 5−9.
(2) Jensen, J. A.; Gozum, J. E.; Pollina, D. M.; Girolami, G. S. *J. Am. Chem. Soc.* **1988**, *110*, 1643−1644.
(3) Sung, J.; Goedde, D. M.; Girolami, G. S.; Abelson, J. R. *Mater. Res. Soc. Symp. Proc.* **1999**, *563*, 39−44.
(4) Sung, J. W.; Goedde, D. M.; Girolami, G. S.; Abelson, J. R. *J. Appl. Phys.* **2002**, *91*, 3904−3911.
(5) Jayaraman, S.; Yang, Y.; Kim, D. Y.; Girolami, G. S.; Abelson, J. R. *J. Vac. Sci. Technol., A* **2005**, *23*, 1619−1625.
(6) Jayaraman, S.; Gerbi, J. E.; Yang, Y.; Kim, D. Y.; Chatterjee, A.; Bellon, P.; Girolami, G. S.; Chevalier, J.-P.; Abelson, J. R. *Surf. Coat. Technol.* **2006**, *200*, 6629−6633.
(7) Yang, Y.; Jayaraman, S.; Kim, D. Y.; Girolami, G. S.; Abelson, J. R. *J. Cryst. Growth* **2006**, *294*, 389−395.
(8) Yang, Y.; Jayaraman, S.; Kim, D. Y.; Girolami, G. S.; Abelson, J. R. *Chem. Mater.* **2006**, *18*, 5088−5096.
(9) Alaux, M. B.; Folcher, G.; Marquet-Ellis, H. U.S. Patent 4,857,294, 1986.
(10) Bridenne, M.; Folcher, G.; Marquet-Ellis, H. *Mater. Sci. Forum* **1985**, *5*, 59−61.
(11) Hirschhorn, I. S.; Tannenbaum, S. U.S. Patent 3,788,798, 1974.
(12) Burg, A. B.; Schlesinger, H. I. *J. Am. Chem. Soc.* **1940**, *62*, 3425−3429.
(13) Schlesinger, H. I.; Brown, H. C. *J. Am. Chem. Soc.* **1953**, *75*, 209−213.
(14) Aldridge, S.; Blake, A. J.; Downs, A. J.; Gould, R. O.; Parsons, S.; Pulham, C. R. *J. Chem. Soc,. Dalton. Trans.* **1997**, 1007−1012.
(15) Hoekstra, H. R.; Katz, J. J. *J. Am. Chem. Soc.* **1949**, *71*, 2488−2492.
(16) Dain, C. J.; Downs, A. J.; Goode, M. J.; Evans, D. G.; Nicholls, K. T.; Rankin, D. W. H.; Robertson, H. E. *J. Chem. Soc., Dalton Trans.* **1991**, 967−977.
(17) Reid, W. E., Jr.; Bish, J. M.; Brenner, A. *J. Electrochem. Soc.* **1957**, *104*, 21−29.
(18) Bird, P. H.; Churchill, M. R. *J. Chem. Soc., Chem. Commun.* **1967**, 403.
(19) Haaland, A.; Shorokhov, D. J.; Tutukin, A. V.; Volden, H. V.; Swang, O.; McGrady, G. S.; Kaltsoyannis, N.; Downs, A. J.; Tang, C. Y.; Turner, J. F. C. *Inorg. Chem.* **2002**, *41*, 6646−6655.
(20) Broach, R. W.; Chuang, I.-S.; Marks, T. J.; Williams, J. M. *Inorg. Chem.* **1983**, *22*, 1081−1084.
(21) Banks, R. H.; Edelstein, N. M.; Rietz, R. R.; Templeton, D. H.; Zalkin, A. *J. Am. Chem. Soc.* **1978**, *100*, 1957−1958.
(22) Banks, R. H.; Edelstein, N. M. In *Lanthanide and Actinide Chemistry and Spectroscopy*; Edelstein, N. M., Ed.; ACS Symposium Series 131; American Chemical Society: Washington, DC, 1980; pp 331−348.
(23) Bernstein, E. R.; Hamilton, W. C.; Keiderling, T. A.; La Placa, S. J.; Lippard, S. J.; Mayerle, J. J. *Inorg. Chem.* **1972**, *11*, 3009−3016.

10.1021/ic0621300 CCC: $37.00
Published on Web 02/16/2007

Np, and Pu are monomeric in the solid state, whereas those of Th, Pa, and U are three-dimensional polymers.

The rarity of monomeric $M(BH_4)_x$ complexes, especially of the transition metals, is a consequence of two factors: the BH_4^- group is a good reductant, and it is sterically small.[26,27] For example, titanium(IV) is reduced by BH_4^- to titanium(III), but volatile $Ti(BH_4)_3$ is unstable and decomposes autocatalytically at room temperature.[15−17,28] Trivalent lanthanides are stable with respect to reduction by BH_4^- but have ionic radii that rival those of the actinides.[29] As a result, complexes such as $Gd(BH_4)_3(DME)$ (DME = 1,2-dimethoxyethane) possess highly polymerized solid-state structures and exhibit low vapor pressures.[30] Homoleptic lanthanide tetrahydroborates are unknown.

The only example of a MB_xH_y complex that does not contain BH_4 ligands is the octahydrotriborate complex $Be(B_3H_8)_2$, which was first characterized in 1975.[31] Metal B_3H_8 complexes that bear ancillary ligands are much more common; for example, the ytterbium species $Yb(B_3H_8)_2(THF)_x$ can be made by treating ytterbium amalgam with BH_3·THF.[32] Structural data for heteroleptic transition-metal complexes containing B_3H_8 ligands[33−40] have shown that the B_3H_8 group is usually bidentate and occupies two mutually cis metal coordination sites. The considerations above led us to ask whether it is possible to prepare new MB_xH_y complexes that contain B_3H_8 ligands. Because B_3H_8 is larger than BH_4, it should be better able to saturate the coordination spheres of transition metals in low oxidation states. As part of our efforts to test this idea, we have recently reported the preparation of the mixed-ligand complexes $(C_5Me_5)Cr(B_3H_8)_2$ and $(C_5Me_5)V(B_3H_8)_2$.[41]

We now describe the synthesis of bis(octahydrotriborato)chromium(II), $Cr(B_3H_8)_2$. This molecule is the first example of a MB_xH_y compound to be described since $Pa(BH_4)_4$, $Np(BH_4)_4$, and $Pu(BH_4)_4$ were reported by Banks et al. in 1978,[21] and it is the first molecular MB_xH_y complex of a transition metal to be discovered since $Ti(BH_4)_3$, $Zr(BH_4)_4$, and $Hf(BH_4)_4$ were reported by Hoekstra and Katz in 1949.[15] We have also synthesized and characterized several Lewis base adducts of $Cr(B_3H_8)_2L_2$ (L = Et_2O, THF, PMe_3) and a volatile purple liquid that we believe is a chromium(III) hydride of stoichiometry $CrH(B_3H_8)_2$. Collectively, these compounds are the first in which there is more than one octahydrotriborate group per transition-metal center. Portions of this work have appeared in preliminary form.[42]

Owing to its volatility, $Cr(B_3H_8)_2$ serves as a chemical vapor deposition precursor for chromium borides, as we have shown elsewhere.[43] The transition-metal borides are of general interest as hard, refractory, and electrically conductive materials.[44]

Results and Discussion

Synthesis of Sodium Octahydrotriborate. The octahydrotriborate anion, $B_3H_8^-$, which is the third member of the hydroborate series (following BH_4^- and $B_2H_7^-$), is an important intermediate in the synthesis of higher boranes.[45,46] The potassium,[45] rubidium,[45] cesium,[45,47] thallium,[48] and tetra(alkyl)ammonium[47,49] salts of $B_3H_8^-$ have been described, and some of these salts have been used to prepare heteroleptic transition-metal B_3H_8 complexes.[31,33−40,50−52] These materials are insoluble in diethyl ether, however, and therefore must be used in solvents such as THF that can coordinate strongly to metal centers. The tetra(alkyl)ammonium salts of $B_3H_8^-$ are soluble in noncoordinating CH_2Cl_2, but this solvent is not always suitable for synthetic purposes, and the separation of the tetra(alkyl)ammonium chloride side product from the desired compound can be problematic. To date, no large-scale synthesis of solvent-free NaB_3H_8 has been reported. The sodium salt has certain advantages over other salts, one of which is that it is soluble in diethyl ether. The development of a larger-scale synthesis could also prove useful in another context; the chemistry of boron hydrides has received increased interest recently, owing to their potential as hydrogen storage materials.[53]

Stock was probably the first to prepare NaB_3H_8 by the direct action of diborane on sodium.[54] Later workers[55,56]

(24) Charpin, P.; Nierlich, M.; Vigner, D.; Lance, M.; Baudry, D. *Acta. Crystallogr., Sect. C* **1987**, *43*, 1465−1467.
(25) Banks, R. H.; Edelstein, N. M.; Spencer, B.; Templeton, D. H.; Zalkin, A. *J. Am. Chem. Soc.* **1980**, *102*, 620−623.
(26) Lobkovskii, E. B. *J. Struct. Chem.* (*Engl. Transl.*) **1983**, *24*, 224−230.
(27) Marks, T. J.; Kolb, J. R. *Chem. Rev.* **1977**, *77*, 263−293.
(28) Franz, K.; Nöth, H. *Z. Anorg. Allg. Chem.* **1973**, *397*, 247−257.
(29) Shannon, R. D. *Acta Crystallogr., Sect. A* **1976**, *32*, 751−767.
(30) Makhaev, V. D.; Borisov, A. P.; Semenenko, K. N. *Russ. J. Inorg. Chem.* (*Engl. Transl.*) **1986**, *31*, 908−910.
(31) Gaines, D. F.; Morris, J. H. *J. Chem. Soc., Chem. Commun.* **1975**, 626−627.
(32) Hill, T. G.; Godfroid, R. A.; White, J. P.; Shore, S. G. *Inorg. Chem.* **1991**, *30*, 2952−2954.
(33) Alcock, N. W.; Burns, I. D.; Claire, K. S.; Hill, A. F. *Inorg. Chem.* **1992**, *31*, 4606−4610.
(34) Grebenik, P. D.; Leach, J. B.; Pounds, J. M.; Green, M. L. H.; Mountford, P. *J. Organomet. Chem.* **1990**, *382*, C1−C5.
(35) Grebenik, P. D.; Leach, J. B.; Green, M. L. H.; Walker, N. M. *J. Organomet. Chem.* **1988**, *345*, C31−C34.
(36) Guggenberger, L. J. *Inorg. Chem.* **1970**, *9*, 367−373.
(37) Lippard, S. J.; Melmed, K. M. *Inorg. Chem.* **1969**, *8*, 2755−2762.
(38) Klanberg, F.; Muetterties, E. L.; Guggenberger, L. J. *Inorg. Chem.* **1968**, *7*, 2272−2278.
(39) Lippard, S. J.; Ucko, D. A. *Inorg. Chem.* **1968**, *7*, 1051−1056.
(40) Muetterties, E. L.; Peet, W. G.; Wegner, P. A.; Alegranti, C. W. *Inorg. Chem.* **1970**, *9*, 2447−2451.
(41) Kim, D. Y.; Girolami, G. S. *J. Am. Chem. Soc.* **2006**, *128*, 10969−10977.
(42) Goedde, D. M.; Girolami, G. S. *J. Am. Chem. Soc.* **2004**, *126*, 12230−12231.
(43) Jayaraman, S.; Klein, E. J.; Yang, Y.; Kim, D. Y.; Girolami, G. S.; Abelson, J. R. *J. Vac. Sci. Technol., A* **2005**, *23*, 631−633.
(44) Matkovich, V. I., Ed. *Boron and Refractory Borides*; Springer-Verlag: New York, 1977.
(45) Hill, T. G.; Godfroid, R. A.; White, J. P.; Shore, S. G. *Inorg. Chem.* **1991**, *30*, 2952−2954.
(46) Titov, L. V.; Eremin, E. R.; Rosolovskii, V. Ya. *Russ. J. Inorg. Chem.* (*Engl. Transl.*) **1982**, *27*, 500−502.
(47) Ryschkewitsch, G. E.; Nainon, K. C.; Dewkett, W. J.; Grace, M.; Beall, H. *Inorg. Synth.* **1974**, *15*, 111−118.
(48) Amberger, E.; Gut, E. *Chem. Ber.* **1968**, *101*, 1200−1204.
(49) Graybill, B. M.; Ruff, J. K.; Hawthorne, M. F. *J. Am. Chem. Soc.* **1961**, *83*, 2669−2670.
(50) Gaines, D. F.; Hildebrandt, S. J. *Inorg. Chem.* **1978**, *17*, 794−806.
(51) Zhang, Y.; Holm, R. H. *Inorg. Chem.* **1990**, *29*, 911−917.
(52) Burns, I. D.; Hill, A. F.; Thompsett, A. R.; Alcock, N. W.; Claire, S. *J. Organomet. Chem.* **1992**, *425*, C8−C10.
(53) Zuttel, A.; Wenger, P.; Rentsch, S.; Sudan, P.; Mauron, P.; Emmenegger, C. *J. Power Sources* **2003**, *118*, 1−7.
(54) Stock, A. *Hydrides of Boron and Silicon*; Cornell University Press: Ithaca, NY, 1933; pp 58 and 138.

discovered that ethers promote this reaction to give a 1:1 mixture of $NaBH_4$ and NaB_3H_8. Solutions of NaB_3H_8 can also be made from $NaBH_4$ and I_2 or $BF_3{\cdot}Et_2O$ in diglyme.[47] This procedure has the advantage of avoiding the use of diborane, but removal of the solvent affords an oil of composition $NaB_3H_8(diglyme)_x$. Solvent-free NaB_3H_8 cannot be obtained directly from this oil because diglyme binds firmly to sodium cations.[57] An indirect method to obtain solvent-free NaB_3H_8, ultimately from $NaB_3H_8(diglyme)_x$, has been described,[58] but this method requires several steps, expensive reagents (sodium tetraphenylborate), and is uneconomical on a large scale.

We have refined a large-scale synthesis of solvent-free NaB_3H_8 by the reaction of sodium amalgam and diborane in diethyl ether. This route uses Brown's method[59] to generate diborane on demand, which is then immediately passed into a flask containing sodium amalgam and diethyl ether at atmospheric pressure.

$$4\ BF_3 + 3\ NaBH_4 \xrightarrow{\text{tetraglyme}} 2\ B_2H_6 + 3\ NaBF_4$$

$$2\ Na/Hg + 2\ B_2H_6 \xrightarrow{Et_2O} NaB_3H_8 + NaBH_4\downarrow + Hg$$

This method permits the synthesis of over 20 g of NaB_3H_8 in one batch. Pure NaB_3H_8 is colorless, air-sensitive, and hygroscopic. It is soluble in water, alcohols, and ethers and is insoluble in pentane, carbon tetrachloride, dichloromethane, and benzene. It decomposes exothermically at 96−100 °C in vacuum[58] but is stable at room temperature.

The ^1H NMR spectrum of NaB_3H_8 shows that the molecule is fluxional at room temperature and that all eight hydrogen atoms are exchanging. Three ^{11}B nuclei ($I = 3/2$) split the ^1H resonance into a 1:3:6:10:12:12:10:6:3:1 decet centered at δ 0.05.[47] The value of $J_{^{11}B-^1H}$ is 33 Hz. The infrared spectrum of NaB_3H_8 shows several $B-H_t$ and $B-H_b$ stretches centered near 2400 and 2100 cm^{-1}, respectively.

Synthesis and Characterization of $CrH(B_3H_8)_2$. Grinding $CrCl_3$ with excess NaB_3H_8 at 20 °C produces a volatile purple liquid, which can be isolated from the reactants by distillation or by extraction with pentane. Pentane extraction is preferred because it is faster and more quantitative. The purple liquid is thermally unstable; neat samples convert to give blue crystals of a chromium(II) species (which will be described below). Pentane solutions of the purple liquid, however, are stable for several hours at room temperature.

The thermal instability and low melting point of the purple liquid have prevented us from carrying out determinations of its absolute elemental composition. We assign the stoichiometry $CrH(B_3H_8)_2$ (**1**) to the purple liquid based on the following evidence. First, the compound contains no chloride, as determined by a silver nitrate test. Second, although a microanalysis of pure samples of **1** was not possible, owing to its thermal instability, we were able to determine that the boron-to-chromium ratio was close to 6:1 by hydrolyzing a pentane solution of **1** and analyzing the hydrolysis products. Third, the infrared spectrum of **1** shows strong terminal B−H bands at 2554 and 2485 cm^{-1} and a strong bridging B−H band at 2005 cm^{-1}, which are consistent with the presence of B_3H_8 groups. Fourth, the purple color and EPR spectrum (see Figure 1) suggest that **1** contains chromium(III). Other methods did not give useful information; no IR band ascribable to a terminal hydride ligand was observed near 1600 cm^{-1}. It is possible that such a band is present but is obscured by the pentane solvent. For comparison, $Cr(BH_4)H(dmpe)_2$[60] (dmpe = $(CH_3)_2PCH_2CH_2P(CH_3)_2$) exhibits a ν_{CrH} band at 1580 cm^{-1}. No molecular ion or fragments thereof were detectable by mass spectrometry (field-ionization and electron-impact ionization); evidently, this molecule is too fragile to survive ionization.[61]

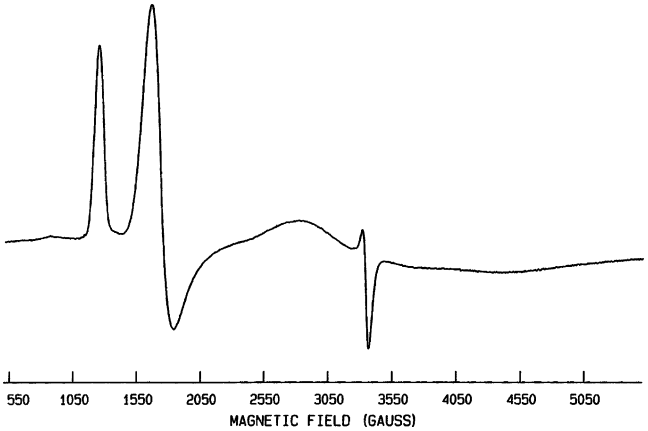

Figure 1. X-band (9.2681 GHz) EPR spectrum of **1**, as a glass in toluene at 77 K.

The X-band EPR spectrum of **1** in a toluene glass at −196 °C (Figure 1) reveals three features at ca. 125, 170, and 330 mT; no hyperfine structure is evident in these absorptions. Analysis of the EPR spectrum was performed by using the Hamiltonian

$$\mathcal{H} = \beta BgS + D[S_z^2 - (1/3)S(S+1) + \lambda(S_x^2 - S_y^2)]$$

where β is the Bohr magneton, S is the spin (here, equal to 3/2), B is the magnetic field strength, g is the Landé g factor, D is a zero-field splitting parameter, and λ is a symmetry parameter that can vary from zero for axial symmetry to one-third for maximum possible rhombic symmetry.[62] In the analysis, g was assumed to be isotropic and equal to 2.00, as usual for high-spin d^3 species.[63,64] The values of $D > 0.4$ cm^{-1} and $\lambda \sim 0.15$ were obtained by matching the observed resonances to calculated transitions using the $D-B$ plot

(55) Hough, W. V.; Edwards, L. J.; McElroy, A. D. *J. Am. Chem. Soc.* **1956**, *78*, 689.
(56) Hough, W. V.; Edwards, L. J.; McElroy, A. D. *J. Am. Chem. Soc.* **1958**, *80*, 1828−1829.
(57) Down, J. L.; Lewis, J.; Moore, B.; Wilkinson, G. *J. Chem. Soc.* **1959**, 3767−3772.
(58) Titov, L. V.; Levicheva, M. D.; Rosolovskii, V. Ya. *Russ. J. Inorg. Chem.* (*Engl. Transl.*) **1980**, *25*, 1625−1627.
(59) Kanth, J. V. B.; Brown, H. C. *Inorg. Chem.* **2000**, *39*, 1795−1802.
(60) Jensen, J. A.; Girolami, G. S. *Inorg. Chem.* **1989**, *28*, 2107−2113.
(61) Similarly, Dain et al. noted that they were not able to determine a meaningful mass spectrum of $Ti(BH_4)_3$ due to its low thermal stability. Dain, C. J.; Downs, A. J.; Goode, M. J.; Evans, D. G.; Nicholls, K. T.; Rankin, D. W. H.; Robertson, H. E. *J. Chem. Soc., Dalton Trans.* **1991**, 967−977.
(62) Dowsing, R. D.; Gibson, J. F. *J. Chem. Phys.* **1969**, *50*, 294−303.

method for $S = 3/2$ spin states.[62,63] The λ parameter, which indicates that the molecule possesses distinct rhombic symmetry, is consistent with the assigned stoichiometry (and inconsistent with a $Cr(B_3H_8)_3$ tris-chelate structure, for which λ should be near zero).

Synthesis and Characterization of $Cr(B_3H_8)_2$. When samples of **1** are kept at room temperature for a few hours, the purple liquid converts into blue needles, which can be isolated by sublimation at 35 °C and 20 mTorr. The blue crystals have the stoichiometry $Cr(B_3H_8)_2$ (**2**). The one-pot reaction of $CrCl_3$ and NaB_3H_8 is not a good method to synthesize **2**; if the purple intermediate **1** is not isolated but instead is allowed to thermolyze in the reaction vessel, only a dark, pyrophoric, and intractable residue results.

The IR spectrum of **2** features strong bands at 2541, 2482, and 2406 cm^{-1} due to terminal B−H stretching vibrations and strong bands at 2131 and 2081 cm^{-1} due to bridging B−H stretching vibrations. The pattern of bands is similar to those seen for bidentate B_3H_8 ligands in other complexes.[49] The magnetic moment of 4.8 μ_B, measured in solution, indicates the presence of four unpaired electrons per chromium center.

The room-temperature ^1H NMR spectrum shows one broad (fwhm = 1800 Hz) resonance at δ 108.5. Owing to the large magnetic moment of the d^4 Cr^{II} center, this peak is unlikely to correspond to hydrogen atoms bound directly to the paramagnetic chromium center. The crystal structure of **2** reveals that the B_3H_8 groups are bidentate, and NMR studies of diamagnetic complexes with bidentate B_3H_8 ligands, such as $(CO)_4Mn(B_3H_8)$ and $(CO)_4Re(B_3H_8)$,[49] show that hydrogen scrambling in B_3H_8 is slow on the NMR time scale at room temperature; in other words, the chemically unique hydrogen positions are discernible. Therefore, we assign the NMR resonance at δ 108.5 to terminal hydrogen atoms on the B atom not bound to Cr.

Crystals of **2** decompose at room temperature within a few days to give a dark mirror on the flask wall. Treatment of **2** with ethylene affords small amounts of polyethylene.

Crystal Structure of $Cr(B_3H_8)_2$. The molecular structure of **2** is illustrated in Figure 2. Crystallographic data and important bond distances and angles for **2** are given in Tables 1 and 2. The chromium center, which lies on a crystallographic inversion center, is ligated by two bidentate $B_3H_8^-$ groups in a square-planar geometry. The Cr−H distances of 1.86(4) and 1.88(5) Å and the Cr−B distance of 2.423(3) Å are similar to those of 1.78(6) and 2.433(3) Å, respectively, seen in $[(CO)_4Cr(B_3H_8)]^-$,[36] and those of 1.89(2) and 2.40(1) Å, respectively, seen for the bidentate B_3H_8 ligand in $Cp^*Cr(B_3H_8)_2$.[41] The ligand bite angle to the chromium center, H_b−Cr−H_b, is 95(2)°. This value is smaller than those seen in the other known complexes containing bidentate B_3H_8 ligands and probably reflects the greater metal−ligand distance present in **2**. The dihedral angle, Cr1−B1−B2/B1−B2−B3, of 120.0(2)° is similar to those seen in other metal B_3H_8 complexes.

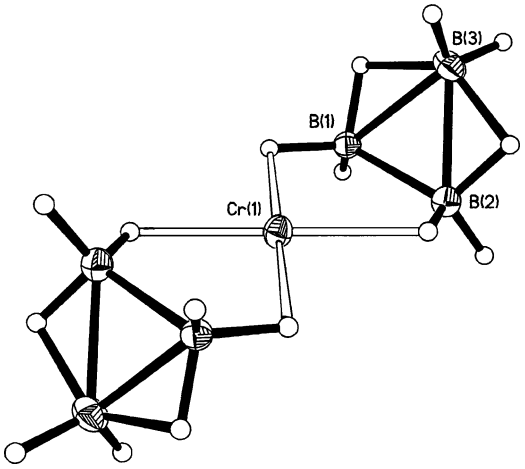

Figure 2. Molecular structure of $Cr(B_3H_8)_2$ (**2**). Ellipsoids are drawn at the 30% probability level, except for hydrogen atoms, which are represented as arbitrarily sized spheres.

There are two intermolecular Cr···H contacts of 2.30(5) Å, each of which involves the chromium center and a terminal hydrogen atom attached to B2 of a neighboring molecule (Figure 3). This interaction provides two long axial ligations to the essentially square-planar chromium atom. It is not surprising that a terminal hydrogen of B1 or B2 (and not B3) interacts with the chromium center of a neighboring molecule; molecular orbital calculations for free $B_3H_8^-$ and $[(CO)_4Cr(B_3H_8)]^-$ indicate that the unique boron atom B3 is more positively charged than B1 and B2.[36] This greater negative charge of B1 and B2 causes the intraligand bridging hydrogens to lie closer to B1 and B2 and farther from B3, 1.16(4) and 1.13(4) Å versus 1.44(4) and 1.43(4) Å. The interaction of the terminal hydrogen H22 with a neighboring chromium center does not lengthen the B−H bond, and the B2−H22 and B1−H12 bonds are equal, within error, at 1.09(4) and 1.03(4) Å, respectively. We believe that the intermolecular Cr···H interactions are weak for the reasons listed, especially because **2** sublimes readily at 35 °C.

Synthesis and Characterization of $Cr(B_3H_8)_2L_2$ Complexes. Interaction of $CrCl_3$ with excess NaB_3H_8 in diethyl ether at 0 °C affords the divalent chromium complex $Cr(B_3H_8)_2(Et_2O)_2$ (**3**), which can be crystallized from diethyl ether at −78 °C in good yield. Crystals of **3** are stable at room temperature under a partial pressure of diethyl ether or under vacuum at −20 °C, but they melt rapidly to a blue oil in the solventless atmosphere of a glovebox or under vacuum at 0 °C.

The diethyl ether ligands of **3** are readily displaced by Lewis bases such as tetrahydrofuran or trimethylphosphine.

$$Cr(B_3H_8)_2(Et_2O)_2 + 2\ L \rightarrow Cr(B_3H_8)_2L_2 + 2\ Et_2O$$
$$\mathbf{4},\ L = THF$$
$$\mathbf{5},\ L = PMe_3$$

The products, $Cr(B_3H_8)_2(THF)_2$ (**4**) and $Cr(B_3H_8)_2(PMe_3)_2$ (**5**), can be crystallized from diethyl ether at −20 °C. Over a few days at room temperature, **5** decomposes to give large

(63) Hempel, J. C.; Morgan, L. O.; Lewis, W. B. *Inorg. Chem.* **1970**, *9*, 2064−2072.
(64) Bonomo, R. P.; Di Bilio, A. J.; Riggi, F. *Chem. Phys.* **1991**, *151*, 323−333 and 385.

Table 1. Crystallographic Data for $Cr(B_3H_8)_2$ (**2**), $Cr(B_3H_8)_2(Et_2O)_2$ (**3**), $Cr(B_3H_8)_2(THF)_2$ (**4**), and $Cr(B_3H_8)_2(PMe_3)_2$ (**5**)

	$Cr(B_3H_8)_2$	$Cr(B_3H_8)_2(Et_2O)_2$	$Cr(B_3H_8)_2(THF)_2$	$Cr(B_3H_8)_2(PMe_3)_2$
T, °C	−75	−75	−75	−75
space group	*P*$\bar{1}$	$P2_1/c$	$P2_1/n$	*Pbca*
a, Å	4.3898(18)	7.0764(17)	9.2051(7)	16.404(3)
b, Å	5.694(2)	16.985(4)	8.7094(6)	13.744(3)
c, Å	9.023(4)	7.985(2)	11.0054(8)	16.728(3)
α, deg	105.192(6)	90	90	90
β, deg	93.810(6)	110.589(4)	102.5340(10)	90
γ, deg	111.102(6)	90	90	90
V, Å^3	199.77(14)	898.4(4)	861.28(11)	3771.6(13)
Z	1	2	4	8
mol wt	132.99	281.23	136.55	285.13
ρ_{calcd}, g cm^{-3}	1.105	1.040	1.053	1.004
λ, Å	0.71073	0.71073	0.71073	0.71073
μ_{calcd}, cm^{-1}	13.16	6.23	4.82	7.49
transm coeff	0.671−0.950	0.700−0.930	0.707−0.914	0.669−0.942
R_F[a]	0.0514	0.0401	0.0351	0.0349
$R_{wF}{}^{2}$[a]	0.1139	0.0733	0.0904	0.0740

[a] $R_F = \sum||F_o| - |F_c||/\sum|F_o|$, $R_{wF}{}^2 = \{\sum[w(F_o{}^2 - F_c{}^2)^2]/\sum[w(F_o{}^2)^2]\}^{1/2}$.

Table 2. Important Bond Lengths (Å) and Angles (deg) for $Cr(B_3H_8)_2$ (**2**)[a]

Bond Lengths			
Cr−B1	2.423(3)	B1−H12	1.03(4)
Cr−B2	2.425(4)	B1−H13	1.16(4)
Cr−H11	1.86(4)	B2−H21	1.07(5)
Cr−H21	1.88(5)	B2−H22	1.09(4)
Cr···H22″	2.30(5)	B2−H23	1.13(4)
B1−B2	1.766(5)	B3−H31	1.13(4)
B1−B3	1.834(5)	B3−H32	1.11(3)
B2−B3	1.834(5)	B3−H13	1.44(4)
B1−H11	1.16(3)	B3−H23	1.43(4)
Bond Angles			
B1−Cr−B2	42.73(12)	H11−B1−H13	102(3)
B1−Cr−B1′	180.00(14)	H12−B1−H13	106(3)
B2−Cr−B2′	180.00(14)	H21−B2−H22	107(3)
B1−Cr−B2′	137.27(12)	H21−B2−H23	100(3)
H11−Cr−H21′	94.6(18)	H22−B2−H23	106(3)
Cr1−B1−H12	123(2)	H31−B3−H32	118(3)
Cr1−B2−H22	121(2)	H31−B3−H13	102(3)
B1−B2−B3	61.2(2)	H31−B3−H23	98(2)
B2−B1−B3	61.2(2)	H32−B3−H13	102(3)
B1−B3−B2	57.6(2)	H32−B3−H23	104(3)
H11−B1−12	106(3)	H13−B3−H23	135(2)

[a] Symmetry related atoms by the transformations ′ = −*x*, 1 − *y*, 1 − *z* and ″ = 1 + *x*, *y*, *z*.

colorless needles of $PMe_3{\cdot}BH_3$, as confirmed by ^{1}H NMR spectroscopy.[65] The purification of **5** by crystallization is made more difficult by the presence of $PMe_3{\cdot}BH_3$, which forms even at −20 °C. Attempts to obtain additional crystal crops of **5** by subliming away the $PMe_3{\cdot}BH_3$ were unsuccessful.

Crystal Structure of $Cr(B_3H_8)_2(Et_2O)_2$. The molecular structure of **3** is illustrated in Figure 4. Crystallographic data, final atomic positions, and important bond distances and angles for **3** are given in Tables 1 and 3, respectively. The chromium center lies on a crystallographic inversion center and is six coordinate; two bidentate $B_3H_8^-$ groups occupy the four equatorial positions, and two diethyl ether molecules occupy the axial positions. The Cr−O distance of 2.059(1) Å is significantly shorter than the axial, intermolecular Cr···H distance of 2.30(5) Å seen for **2**. The chromium−boron distances for **3**, which average 2.609 Å, are longer than the same distances in **2** by nearly 0.2 Å. The Cr−H_b distances of 1.98(2) and 1.99(2) Å are significantly longer than those in $[(CO)_4Cr(B_3H_8)]^-$ [36] and slightly longer than

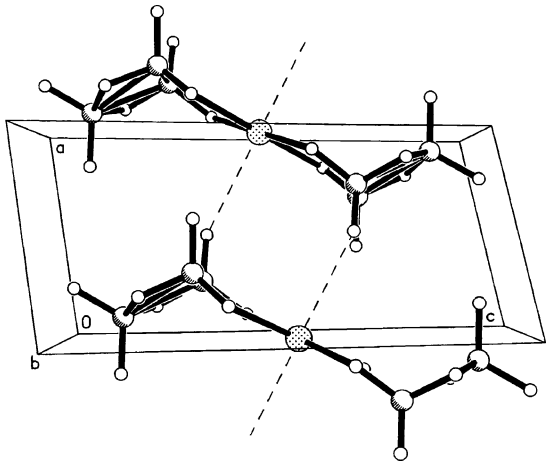

Figure 3. View showing the 2.30(5) Å Cr···H intermolecular contacts in $Cr(B_3H_8)_2$ (**2**). The atoms are represented by arbitrarily sized spheres.

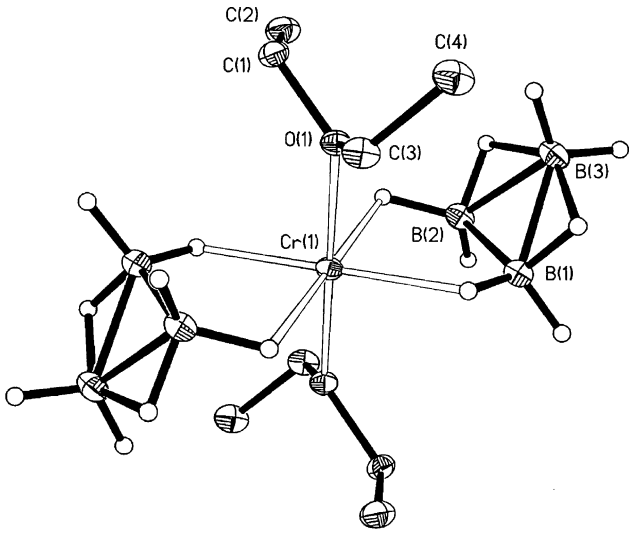

Figure 4. Molecular structure of $Cr(B_3H_8)_2(Et_2O)_2$ (**3**). Ellipsoids are drawn at the 30% probability level, except for hydrogen atoms, which are represented as arbitrarily sized spheres.

(65) Cowley, A. H.; Damasco, M. C. *J. Am. Chem. Soc.* **1971**, *93*, 6815−6821.

Table 3. Important Bond Lengths (Å) and Angles (deg) for Cr(B$_3$H$_8$)$_2$(Et$_2$O)$_2$ (**3**)[a]

Bond Lengths			
Cr−O	2.0591(13)	B1−H12	1.06(2)
Cr−B1	2.627(3)	B1−H13	1.11(2)
Cr−B2	2.591(3)	B2−H21	1.149(19)
Cr−H11	1.99(2)	B2−H22	1.05(2)
Cr−H21	1.981(18)	B2−H23	1.13(2)
B1−B2	1.791(4)	B3−H31	1.06(2)
B1−B3	1.814(3)	B3−H32	1.07(2)
B2−B3	1.821(4)	B3−H13	1.39(2)
B1−H11	1.16(2)	B3−H23	1.47(2)
Bond Angles			
O−Cr−O′	180	B1−B2−B3	60.29(14)
O−Cr−B1	90.41(7)	B2−B1−B3	60.66(14)
O−Cr−B2	94.70(7)	B1−B3−B2	59.05(13)
O−Cr−H11	82.5(6)	H11−B1−H12	115.1(15)
O−Cr−H21	89.6(6)	H11−B1−H13	100.6(16)
O′−Cr−B1	89.59(7)	H12−B1−H13	104.4(17)
O′−Cr−B2	85.30(7)	H21−B2−H22	112.9(16)
O′−Cr−H11	97.5(6)	H21−B2−H23	96.6(16)
O′−Cr−H21	90.4(5)	H22−B2−H23	109.6(17)
B1−Cr−B2	40.14(8)	H31−B3−H32	117.9(16)
B1−Cr−B1′	180	H31−B3−H13	103.0(15)
B2−Cr−B2′	180	H31−B3−H23	102.5(15)
B1−Cr−B2′	139.86(8)	H32−B3−H13	103.2(15)
H11−Cr−H21	87.5(8)	H32−B3−H23	96.6 1(5)
Cr1−B1−H12	127.0(11)	H13−B3−H23	135.1(14)
Cr1−B2−H22	118.2(12)		

[a] Primed atoms generated from unprimed atoms by the transformation $1 - x$, $1 - y$, $1 - z$.

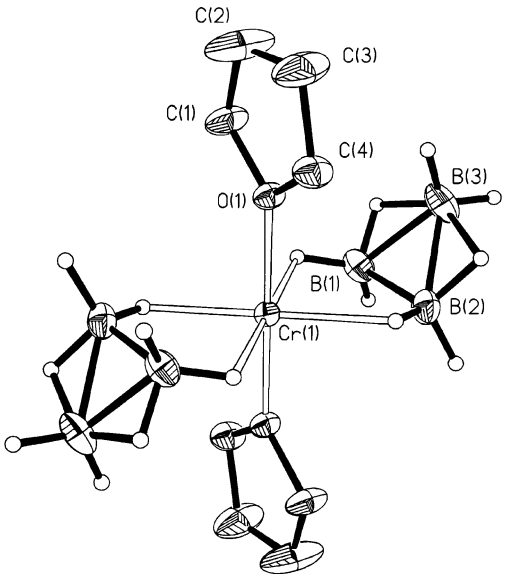

Figure 5. Molecular structure of Cr(B$_3$H$_8$)$_2$(THF)$_2$ (**4**). Ellipsoids are drawn at the 30% probability level, except for hydrogen atoms, which are represented as arbitrarily sized spheres.

those of 1.87(5) Å in homoleptic Cr(B$_3$H$_8$)$_2$. The Cr−H$_b$ distances are equal within experimental error; the square plane is defined by the four Cr−H$_b$ contacts.

Crystal Structure of Cr(B$_3$H$_8$)$_2$(THF)$_2$. The molecular structure of **4** is illustrated in Figure 5. Crystallographic data, final atom positions, and important bond distances and angles for **4** are given in Tables 1 and 4, respectively. The chromium center lies on a crystallographic inversion center and is six coordinate with two bidentate B$_3$H$_8^-$ groups and two mutually trans tetrahydrofuran molecules. The Cr−O distance

Table 4. Important Bond Lengths (Å) and Angles (deg) for Cr(B$_3$H$_8$)$_2$(THF)$_2$ (**4**)[a]

Bond Lengths			
Cr−O	2.0182(12)	B1−H12	1.13(2)
Cr−B1	2.565(2)	B1−H13	1.26(2)
Cr−B2	2.580(2)	B2−H21	1.170(12)
Cr−H11	1.90(2)	B2−H22	1.17(2)
Cr−H21	1.977(19)	B2−H23	1.19(2)
B1−B2	1.801(4)	B3−H31	1.18(3)
B1−B3	1.814(4)	B3−H32	1.17(3)
B2−B3	1.812(4)	B3−H13	1.39(2)
B1−H11	1.24(2)	B3−H23	1.42(2)
Bond Angles			
O−Cr−O′	180	B1−B2−B3	60.28(15)
O−Cr−B1	92.68(7)	B2−B1−B3	60.18(15)
O−Cr−B2	92.77(7)	B1−B3−B2	59.55(15)
O−Cr−H11	83.8(6)	H11−B1−H12	119.3(14)
O−Cr−H21	85.6(5)	H11−B1−H13	97.3(14)
O′−Cr−B1	87.32(7)	H12−B1−H13	107.7(14)
O′−Cr−B2	87.23(7)	H21−B2−H22	113.5(15)
O′−Cr−H11	92.6(6)	H21−B2−H23	102.6(14)
O′−Cr−H21	94.4(5)	H22−B2−H23	102.4(15)
B1−Cr−B2	40.97(8)	H31−B3−H32	122.2(19)
B1−Cr−B1′	180	H31−B3−H13	102.0(16)
B2−Cr−B2′	180	H31−B3−H23	91.4(15)
H11−Cr−H21	91.2(9)	H32−B3−H13	99.6(15)
Cr1−B1−H12	124.9(10)	H32−B3−H23	100.9(14)
Cr1−B2−H22	122.5(11)	H13−B3−H23	144.2(14)

[a] Primed atoms generated from unprimed atoms by the transformation $-x$, $-y$, $-z$.

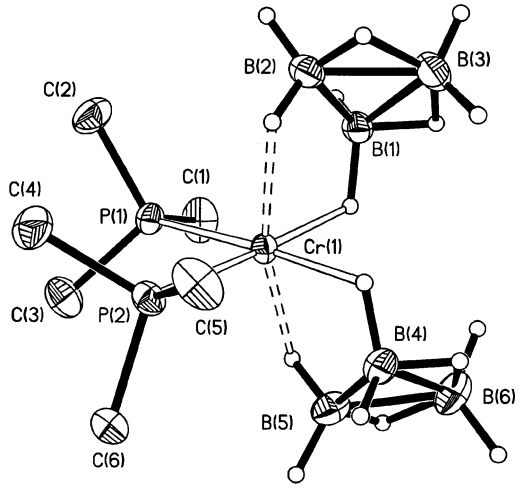

Figure 6. Molecular structure of Cr(B$_3$H$_8$)$_2$(PMe$_3$)$_2$ (**5**). Ellipsoids are drawn at the 30% probability level, except for hydrogen atoms, which are represented as arbitrarily sized spheres.

of 2.018(1) Å for **4** is slightly shorter than the corresponding distance seen in **3**. The two Cr−B distances for **4** differ from each other slightly, 2.565(2) and 2.580(2) Å. In compounds **2** and **3**, the Cr−B distances are ∼0.15 Å shorter and ∼0.04 Å longer, respectively. The two Cr−H$_b$ distances in **4** are nearly identical within error at 1.90(2) and 1.98(2) Å.

Crystal Structure of Cr(B$_3$H$_8$)$_2$(PMe$_3$)$_2$. The molecular structure of **5** is illustrated in Figure 6. Crystallographic data, final atom positions, and important bond distances and angles for **5** are given in Tables 1 and 5, respectively. The geometry about chromium is a tetragonally elongated octahedron; the two PMe$_3$ ligands occupy mutually cis positions in the equatorial plane. A noncrystallographic C_2 axis passes through the chromium center and bisects the P−Cr−P angle.

Table 5. Important Bond Lengths (Å) and Angles (deg) for $Cr(B_3H_8)_2(PMe_3)_2$ (**5**)

Bond Lengths			
Cr−P1	2.4772(7)	B5−B6	1.802(5)
Cr−P2	2.4659(7)	B1−H11	1.187(18)
P1−C1	1.814(2)	B1−H12	1.06(2)
P1−C2	1.811(2)	B1−H13	1.17(2)
P1−C3	1.812(2)	B2−H21	1.152(19)
P2−C4	1.819(2)	B2−H22	1.05(2)
P2−C5	1.815(2)	B2−H23	1.12(2)
P2−C6	1.809(2)	B3−H31	1.08(2)
Cr−B1	2.529(2)	B3−H32	1.04(2)
Cr−B2	2.645(3)	B3−H13	1.43(2)
Cr−H11	1.878(19)	B3−H23	1.42(2)
Cr−H21	2.060(19)	B4−H41	1.218(18)
Cr−B4	2.507(3)	B4−H42	1.10(2)
Cr−B5	2.633(3)	B4−H43	1.14(3)
Cr−H41	1.850(18)	B5−H51	1.13(2)
Cr−H51	2.13(2)	B5−H52	1.08(2)
B1−B2	1.784(3)	B5−H53	1.12(3)
B1−B3	1.807(4)	B6−H61	1.10(3)
B2−B3	1.813(4)	B6−H62	1.11(3)
B4−B5	1.781(4)	B6−H43	1.36(3)
B4−B6	1.818(4)	B6−H53	1.40(3)
Bond Angles			
P1−Cr−P2	94.97(2)	H12−B1−H13	105.6(16)
P1−Cr−H11	91.5(5)	H21−B2−H22	116.3(14)
P1−Cr−H21	104.0(5)	H21−B2−H23	100.8(15)
P1−Cr−H41	173.4(6)	H22−B2−H23	105.3(15)
P1−Cr−H51	83.6(6)	H31−B3−H32	118.1(16)
P2−Cr−H11	171.4(5)	H31−B3−H13	99.3(13)
P2−Cr−H21	83.7(5)	H31−B3−H23	104.5(14)
P2−Cr−H41	88.8(5)	H32−B3−H13	96.2(15)
P2−Cr−H51	109.3(5)	H32−B3−H23	102.6(15)
H11−Cr−H21	89.2(8)	H13−B3−H23	137.5(14)
H11−Cr−H41	85.3(7)	B4−Cr−B5	40.45(9)
H11−Cr−H51	77.1(7)	B4−B5−B6	60.97(18)
H21−Cr−H41	81.8(8)	B5−B4−B6	60.08(18)
H21−Cr−H51	164.6(8)	B4−B6−B5	58.95(16)
H41−Cr−H51	90.0(8)	H41−B4−H42	110.9(13)
Cr−P1−C1	110.35(8)	H41−B4−H43	98.1(16)
Cr−P1−C2	117.75(8)	H42−B4−H43	111.9(19)
Cr−P1−C3	116.96(8)	H51−B5−H52	113.5(15)
Cr−P2−C4	115.95(8)	H51−B5−H53	96.7(17)
Cr−P2−C5	111.47(8)	H52−B5−H53	103.9(18)
Cr−P2−C6	116.27(7)	H61−B6−H62	121.2(18)
B1−Cr−B2	40.25(7)	H61−B6−H43	98.1(17)
B1−B2−B3	60.32(14)	H61−B6−H53	104.0(17)
B2−B1−B3	60.65(15)	H62−B6−H43	96.0(17)
B1−B3−B2	59.03(14)	H62−B6−H53	103.8(17)
H11−B1−H12	110.9(13)	H43−B6−H53	136.2(17)
H11−B1−H13	98.0(14)		

Whereas the B_3H_8 ligands of **2**, **3**, and **4** are bound to the metal in a symmetrical fashion (i.e., the M−H_b and M−B distances are nearly identical for each ligand), the B_3H_8 ligands of **5** are bound in an unsymmetrical fashion. The two $B_3H_8^-$ groups each possess one short equatorial Cr−B bond and one, longer, axial bond; the Cr−B distances are 2.529(2) and 2.507(3) Å (equatorial) versus 2.645(3) and 2.633(3) Å (axial). The Cr−H equatorial and axial distances are similarly unequal at 1.85(2) and 1.88(2) Å versus 2.06(2) and 2.13(2) Å, respectively. Unlike the structures of the diethyl ether and tetrahydrofuran adducts **3** and **4**, it is clear that, in **5**, the square plane encompasses the two Lewis bases and the two short Cr−H_b bonds.

Interestingly, the diethyl ether ligands in **3** and the tetrahydrofuran ligands in **4** are bound at axial, mutually trans sites, whereas the PMe_3 ligands of **5** occupy mutually cis positions in the equatorial plane. This latter arrangement can be explained by crystal field theory. These high-spin d^4 complexes possess only one vacant metal d orbital: $d_{x^2-y^2}$. The strong-field PMe_3 ligand is better able to lower the energy of the metal−ligand bonding orbitals than $B_3H_8^-$; therefore, PMe_3 occupies the equatorial plane where it can overlap strongly with the $d_{x^2-y^2}$ orbital. Structures **2**−**5**, as a result, demonstrate that the σ-donor abilities of the following ligands fall in the following order $PMe_3 > B_3H_8^- > THF \sim Et_2O$.

Steric Analysis of B_3H_8 Complexes. Lobkovskii has presented a simple and effective algorithm for estimating the steric saturation of metal complexes, which uses a type of normalized solid angle.[26] For each ligand L in a complex, a steric constant S_L (in units of Å^2) is divided by r^2, r being the metal−ligand distance in Å. The quotients for all of the ligands in the complex are summed, and a sum near unity corresponds to a full coordination sphere. From the structures of $Cr(B_3H_8)_2(Et_2O)_2$ and $Cr(B_3H_8)_2(THF)_2$, and Lobkovskii's finding that S_{THF} and S_{Et_2O} both equal 0.80 Å^2, we can estimate that S_L for a bidentate $B_3H_8^-$ ligand is 1.95 Å^2. This knowledge may aid in the design of other volatile $M(B_xH_y)_n$ molecules suitable as precursors to metal boride phases by chemical vapor deposition.

Experimental Section

All operations were carried out in vacuum or under argon by using standard Schlenk techniques.[66] Diethyl ether and pentane were distilled under nitrogen from sodium benzophenone immediately before use. Tetraethylene glycol dimethyl ether (tetraglyme) (Aldrich, 99%) was vacuum distilled from molten sodium. Boron trifluoride diethyl etherate (Aldrich) was vacuum distilled from CaH_2. Triply distilled mercury (Bethlehem Apparatus Co.), sodium metal (Aldrich), and $NaBH_4$ (Aldrich, 98%) were used as received. Anhydrous $CrCl_3$ was prepared from $[Cr(H_2O)_4Cl_2]Cl\cdot 2H_2O$ by a literature method.[67]

Microanalyses were performed by the University of Illinois Microanalytical Laboratory. The IR spectra were recorded on a Nicolet Impact 410 instrument as Nujol mulls or as a solution in Nujol, pentane, or toluene. The proton and phosphorus NMR data were collected on a Varian Gemini 400 instrument at 399.953 and 161.903 MHz, respectively. Chemical shifts are reported in δ units (positive shifts to high frequency) relative to tetramethylsilane (^{1}H) or 85% H_3PO_4 (^{31}P). Magnetic moments were determined in C_6D_6 by the Evans NMR method.[68] Melting points were determined in closed capillaries under argon on a Thomas−Hoover Unimelt apparatus or, in the case of $Cr(B_3H_8)_2(Et_2O)_2$ (**3**), in a closed flask under argon.

Sodium Octahydrotriborate, NaB_3H_8. ***Caution!*** *Boron trifluoride diethyl etherate is toxic and flammable. Diborane is a toxic gas that ignites spontaneously in contact with air. Diethyl ether is flammable. Sodium metal reacts explosively with water. Mercury is toxic. This procedure should be carried out in an efficient hood with explosion shields in place.*

A drawing of the experimental apparatus is given in Figure 7. Krytox LVP (DuPont) fluorinated grease was used on all ground-glass joints. All tubing used was Nalgene with a 1/16 in. wall

(66) Shriver, D. F.; Drezdzon, M. A. *The Manipulation of Air-Sensitive Compounds*, 2nd ed.; Wiley: New York, 1986.
(67) Pray, A. R. *Inorg. Synth.* **1990**, *28*, 321−323.
(68) Evans, D. F.; Fazakerley, G. V.; Phillips, R. F. *J. Chem. Soc. A* **1971**, 1931−1934.

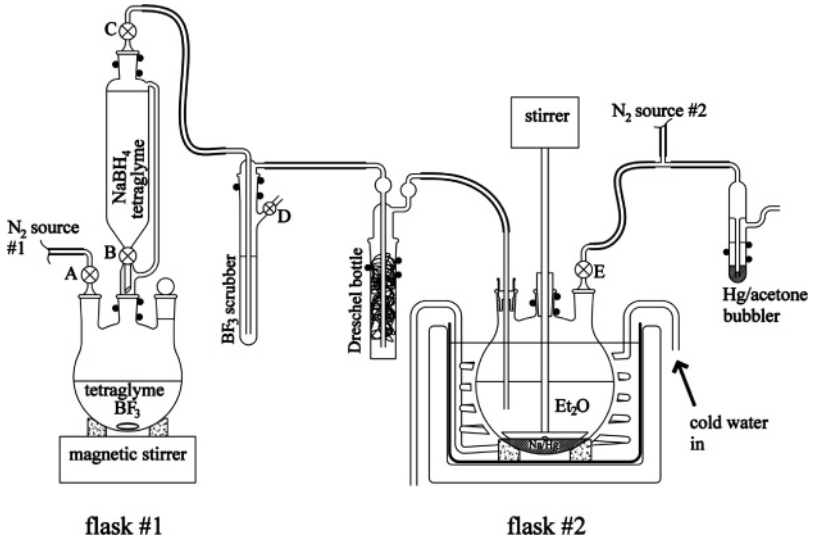

Figure 7. Schematic drawing of the apparatus used to synthesize NaB_3H_8. Clamp locations are indicated by three black dots.

thickness. Glassware was oven-dried overnight, assembled hot, and allowed to cool under nitrogen.

A 4 M solution of boron trifluoride in tetraglyme was prepared by adding tetraglyme (650 mL) to boron trifluoride diethyl etherate (369 mL, 2.91 mol) and then removing the freed diethyl ether under vacuum at room temperature to give approximately 725 mL of a yellow or brown liquid.

A three-necked 2 L flask (flask #1) is supported on a cork ring above a magnetic stirrer, charged with a Teflon-coated magnetic stir bar, and fitted with a gas adapter (A), a pressure-equalized dropping funnel (800 mL), and a septum in the right neck. A septum is loosely inserted in joint C at the top of the dropping funnel. While still hot, flask #1 is flushed with nitrogen from A out through C. Flask #1 is charged with the previously prepared BF_3·tetraglyme solution by means of a 4 mm Teflon cannula that passes through the septum in the right neck. The septum in the right neck is then replaced with a ground-glass stopper. ***Caution!*** *Ensure that stopcock B is closed before proceeding.* A 3 M solution of $NaBH_4$ (89.5 g, 2.37 mol) in tetraglyme (790 mL) is transferred to the dropping funnel by means of a 4 mm Teflon cannula that passes through the septum in joint C. The septum in joint C is replaced with a gas adapter. Stopcocks A and C are then closed.

A three-necked 3 L flask (flask #2) is fitted with a septum in the left neck, a Teflon-paddle mechanical stirrer sealed by a Trubore adapter in the center neck, and a gas adapter (E) in the right neck. A cork ring is used to support flask #2 in a polyethylene bucket. Copper tubing (1 cm outer diameter) is wound into a coil (20 cm diameter) and placed in the polyethylene bucket around flask #2. A T tube connects E to a nitrogen gas line and to a bubbler, which contains a 3 cm tall column of mercury covered with acetone. Flask #2 is flushed with nitrogen from E by loosening the septum in the left neck. After flask #2 has cooled, mercury (372 mL, 5.0 kg) is slowly added against a gentle stream of nitrogen. Sodium (39.8 g, 1.73 mol) is added as small pieces to the stirred mercury over 1 h so that the amalgam becomes warm (ca. 50 °C) but not hot. After the amalgam has cooled to room temperature, kerosene is added to the bucket until most of flask #2 is immersed. Degassed diethyl ether (1.5 L) is added to flask #2 by means of cannula through the septum in the left neck. The polyethylene bucket is wrapped with glass wool.

The left neck of flask #2 is plugged with a septum while a BF_3 scrubber is assembled. The BF_3 scrubber consists of a 100 mL trap equipped with a stopcock sidearm (D); the scrubber is charged with a 2 M solution of $NaBH_4$ (3.7 g) in tetraglyme (50 mL). Against a gentle stream of nitrogen from flask #1, the BF_3 scrubber is connected to C with a section of hose. A Dreschel bottle (packed loosely with oven-dried glass wool) is attached to the outlet of the BF_3 scrubber with a section of hose. (The Dreschel bottle and glass wool packing filters out any tetraglyme aerosols and also serves as a backup in case the BF_3 scrubber overflows. Cotton should not be used as a filter because it reacts with diborane.) A 25 cm long, 6 mm outer diameter Pyrex glass tube is pushed through a septum with a small circular hole so as to achieve a tight glass−septum fit. The exit of the Dreschel bottle is connected by hose to the Pyrex tube. After the BF_3 scrubber and Dreschel bottle have been flushed with N_2 for 20 min, the septum with the Pyrex tube is firmly seated into the left neck of flask #2 with the end of the glass tube adjusted several centimeters below the surface of the diethyl ether. The entire assembled apparatus is flushed for 10 min from A, allowing nitrogen to exit the mercury/acetone bubbler. Finally, copper tubing (6 mm outer diameter, 5 m length) wound into coils is placed into a 20 L bucket, and then, the bucket is filled with ice. Nalgene tubing (3/8 in. diameter) is used to connect a source of tap water to the 5 m coil, the 5 m coil to the coil in the polyethylene bucket, and the exit of the coil in the polyethylene bucket to a sink drain. A slow flow of tap water (300 mL/min) typically achieves a kerosene bath temperature of 4−6 °C.

After flask #2 is cooled to 4−6 °C and the magnetic and mechanical stirrers have been set into motion, nitrogen source #2 and A are closed. B is opened slightly to deliver 1 drop of $NaBH_4$ solution every 4−6 s. The generated diborane initially displaces the inert blanketing gas from the apparatus through the mercury/acetone bubbler. After the first 2−3 h of diborane generation, the $NaBH_4$ solution is added to the BF_3 solution as fast as possible, but not so fast that B_2H_6 escapes through the bubbler (if the addition is too fast, the acetone in the bubbler will become warm as it reacts with the escaping diborane). The total time for the $NaBH_4$ addition is typically 24−36 h. After all of the $NaBH_4$ solution has been added to the BF_3 solution, the mechanical and magnetic stirrers are allowed to operate for an additional 8 h, and then, the entire system is flushed for 4 h with nitrogen from A.

The contents of flask #2 are allowed to settle, nitrogen source #2 is attached directly to E, and the diethyl ether supernatant is filtered into a 3 L flask through No. 1 Whatman filter paper by means of a filter cannula. The remaining gray solids are extracted four times with degassed diethyl ether (250 mL). The diethyl ether

extracts are filtered and combined with the original supernatant. The resulting solution is concentrated to ca. 250 mL by distillation under nitrogen, and then, the concentrate is transferred by cannula to a 500 mL flask. Vacuum removal of the diethyl ether at room temperature over 4 h produces a white solid that coats the flask walls. The white solid is maintained under dynamic vacuum overnight and then scraped down off the walls under nitrogen, washed with degassed pentane (2 × 100 mL), and dried under vacuum (1 h) to give NaB_3H_8 (25.5 g, 55% yield based on $BF_3 \cdot Et_2O$). Anal. Calcd for NaB_3H_8: Na, 36.2; B, 51.1; H, 12.7. Found: Na, 34.0; B, 53.6; H, 12.8. ^{1}H NMR (tetrahydrofuran-d_8): δ 0.05 (decet, 8H, J_{11B-H} = 33 Hz). IR (cm^{-1}): 2472 (s), 2424 (s), 2400 (sh), 2361 (s), 2334 (s), 2131 (m), 2098 (m), 1173 (s), 1007 (s), 791 (w), 738 (w), 443 (m).

Regeneration of Materials. After the generation of diborane in flask #1 has been completed, $NaBF_4$ is essentially the only solute dissolved in the tetraglyme. $NaBF_4$ is soluble in tetraglyme at room temperature but is much less soluble above 100 °C.[65] The solution is stirred and slowly heated to 150 °C under a purge of nitrogen, which sweeps the small amounts of liberated diborane out of the flask and into the hood. This temperature is maintained overnight while colorless crystals of $NaBF_4$ accumulate on the flask wall. While hot, the tetraglyme is decanted from the $NaBF_4$ by cannula and readied for reuse by vacuum distillation from molten sodium.

After the NaB_3H_8 has been removed, flask #2 contains $NaBH_4$ and spent amalgam. Cold water is slowly added to flask #2 against a stream of nitrogen. The aqueous solution of $NaBH_4$ is slowly acidified with dilute HCl until gas evolution subsides. The aqueous layer is discarded, and traces of HCl are removed from the mercury by washing with water. The mercury is then readied for reuse by drying under vacuum at room temperature.

(Hydrido)bis(octahydrotriborato)chromium(III), $CrH(B_3H_8)_2$. Method A. A mixture of $CrCl_3$ (0.45 g, 2.8 mmol) and NaB_3H_8 (0.82 g, 13 mmol) was placed in a 250 mL round-bottomed flask, and 100 steel balls (4.5 mm diameter) were added. The flask was gently agitated by hand for 15 min; and over this period, gas evolved and the reactant powders became damp and changed color to dark purple. The purple product was transferred under vacuum into a flask cooled to −196 °C. Yield: approximately 0.5 mL of purple liquid. Mp: below −20 °C. EPR (toluene, −196 °C): three features at 125, 170, and 330 mT. IR (pentane, cm^{-1}): 2588 (sh), 2568 (sh), 2554 (vs), 2541 (sh), 2485 (vs), 2261 (w), 2131 (m), 2068 (w), 2005 (vs br), 1160 (w), 1135 (m), 1040 (w), 996 (m), 972 (m br), 872 (m br), 819 (s br), 620 (m br).

Method B. A mixture of $CrCl_3$ (1.49 g, 9.41 mmol) and NaB_3H_8 (1.89 g, 29.8 mmol) was treated as described in Method A. However, instead of carrying out a vacuum transfer, the purple liquid was extracted from the reaction flask with pentane (2 × 80 mL). The extracts were filtered, combined, and the pentane was removed under vacuum at 0 °C to afford a purple liquid.

Method C. To a mixture of $CrCl_3$ (0.46 g, 2.9 mmol) and NaB_3H_8 (0.80 g, 13 mmol) at room temperature were added a Teflon magnetic stir bar, 40 Pyrex spheres (3 mm diameter), and pentane (30 mL). As the slurry was stirred rapidly, gas evolved, and the solution color became purple. After 3 h, the solution was filtered, and the residue was washed with pentane (5 × 30 mL). The washings were filtered and combined with the original solution, and the solvent was removed under vacuum at 0 °C to afford a purple liquid. The B/Cr ratio was determined in the following manner. Deionized water (20 mL) was added to a 100 mL argon-filled flask by syringe and then frozen by cooling to −78 °C. A small amount of **1** in pentane (ca. 0.5 mL) was layered above the ice, and a ground-glass stopper sealed the flask. The flask contents were allowed to warm to room temperature with agitation. The solution was transferred to a 100 mL volumetric Teflon flask with washings of 6 M HCl in deionized water. Additional HCl solution was added to the volumetric flask to bring the total volume to 100 mL. The hydrolyzed sample of **1** was analyzed by ICP elemental analysis to contain 317.2 μg of boron and 246.7 μg of Cr; the relative B/Cr atomic ratio was 6.18:1.00. Addition of Ag^+ to another hydrolyzed sample of **1** gave a negative test for chloride.

Bis(octahydrotriborato)chromium(II), $Cr(B_3H_8)_2$. A sample of **1**, prepared from $CrCl_3$ (1.49 g, 9.41 mmol) and NaB_3H_8 (1.89 g, 29.8 mmol) by method B described previously, was freed of excess pentane under vacuum at 0 °C and then stored under argon at room temperature until conversion to blue crystals was complete (ca. 3 h). Blue crystals of $Cr(B_3H_8)_2$ at 0 °C were washed with pentane (2 × 10 mL) and purified by sublimation (35 °C, 20 mTorr). Yield: 0.296 g (24% based on Cr). Mp: 64 °C (dec). Anal. Calcd for $B_6H_{16}Cr$: H, 12.1; B, 48.8; Cr, 39.1. Found: H, 11.3; B, 46.6; Cr, 38.9. ^{1}H NMR (C_6D_6, 20 °C): δ 108.5 (s, fwhm = 1800 Hz, see text for assignment). Magnetic moment (benzene, 20 °C): 4.8 μ_B. IR (Nujol, cm^{-1}): 2557 (m), 2541 (s), 2515 (m), 2504 (m), 2489 (sh), 2482 (s), 2432 (sh), 2406 (s), 2269 (w), 2155 (sh), 2131 (s), 2081 (s br), 2017 (sh), 1307 (w), 1266 (w), 1207 (w), 1168 (m), 1140 (m), 1054 (w), 1020 (sh), 1009 (s), 973 (s), 918 (sh), 889 (w), 869 (m), 769 (m), 731 (s), 666 (m), 632 (s br), 510 (m).

Bis(octahydrotriborato)bis(diethylether)chromium(II), $Cr(B_3H_8)_2(Et_2O)_2$. To a suspension of $CrCl_3$ (0.86 g, 5.4 mmol) in diethyl ether (20 mL) at 0 °C was added a solution of NaB_3H_8 (1.30 g, 20.5 mmol) in diethyl ether (20 mL). The slurry was stirred at 0 °C for 3 h; over this period, gas slowly evolved and the originally purple solution became dull green. The solvent was removed at 0 °C, and the residue was extracted with pentane (70 mL). The extract was filtered into a flask cooled to 0 °C, and the solvent was removed under vacuum. The residue was extracted with diethyl ether (10 mL), and the green extract was filtered and cooled to −78 °C to afford blue crystals, which were dried under vacuum at −20 °C. Yield: 0.98 g (64%). Mp: 39 °C. ^{1}H NMR (C_6D_6, 20 °C): δ 28.4 (s, fwhm = 1200 Hz, CH_2), 12.2 (s, fwhm = 530 Hz, CH_3). Magnetic moment (benzene, 20 °C): 4.4 μ_B. IR (Nujol, cm^{-1}): 2515 (s), 2459 (s), 2372 (w), 2343 (w), 2153 (s br), 2105 (s br), 1303 (w), 1262 (w), 1183 (w), 1148 (m), 1089 (m), 1028 (s), 1011 (sh), 976 (w), 899 (m), 865 (w), 830 (m), 777 (m), 616 (m br), 513 (w).

Bis(octahydrotriborato)bis(tetrahydrofuran)chromium(II), $Cr(B_3H_8)_2(THF)_2$. A sample of $Cr(B_3H_8)_2(Et_2O)_2$ (0.70 g, 2.5 mmol) was dissolved in tetrahydrofuran (10 mL) at −78 °C, and the solution was warmed to room temperature over 10 min to give a pastel-blue slurry. The solvent was removed under vacuum, and the residue was extracted with diethyl ether (4 × 15 mL). The extracts were filtered, combined, and cooled to −20 °C to afford blue crystals. Yield: 0.55 g (80%). Mp: 92 °C (dec). Anal. Calcd for $C_8H_{32}B_6O_2Cr$: C, 34.7; H, 11.6; B, 23.4; Cr, 18.8. Found: C, 34.8; H, 11.5; B, 21.9; Cr, 19.1. ^{1}H NMR (C_7D_8, 20 °C): δ 66 (s, fwhm = 3200 Hz, β-CH_2). Magnetic moment (benzene, 20 °C): 4.6 μ_B. IR (Nujol, cm^{-1}): 2515 (sh), 2496 (s), 2483 (s), 2445 (s), 2352 (w), 2279 (w), 2205 (s br), 2114 (m br), 1889 (w), 1246 (w), 1170 (m), 1147 (m), 1102 (w), 1039 (m), 1015 (s), 974 (m), 922 (m), 864 (s br), 816 (m br), 724 (s), 696 (w), 619 (s br), 501 (w), 422 (s).

Bis(octahydrotriborato)bis(trimethylphosphine)chromium(II), $Cr(B_3H_8)_2(PMe_3)_2$. To $CrCl_3$ (0.66 g, 4.15 mmol) suspended in diethyl ether (20 mL) at 0 °C was added a solution of NaB_3H_8 (0.848 g, 13.4 mmol) in diethyl ether (20 mL). The mixture was stirred at 0 °C for 3 h. The resulting blue solution was cooled to

−78 °C and treated with PMe_3 (0.90 mL, 8.7 mmol). A turquoise-colored precipitate formed immediately. As the solution was warmed to room temperature, all of the precipitate dissolved. The solution was concentrated to ∼25 mL under vacuum and then cooled to −20 °C to afford deep blue crystals. Yield: 0.306 g (26%). Mp: 65 °C. Anal. Calcd for $C_6H_{34}B_6P_2Cr$: C, 25.3; H, 12.0; B, 22.8; P, 21.7; Cr, 18.2. Found: C, 25.0; H, 11.5; B, 21.9; P, 19.8; Cr, 17.9. ^{1}H NMR (C_7D_8, 20 °C): δ −23.2 (s, fwhm = 931 Hz, PMe_3). ^{31}P{^{1}H} NMR (C_7D_8, 20 °C): δ 126 (s, fwhm = 1830 Hz, PMe_3). Magnetic moment (benzene, 20 °C): 4.5 μ_B. IR (Nujol, cm^{-1}): 2509 (sh), 2499 (s), 2486 (s), 2465 (s), 2441 (s), 2430 (s), 2412 (sh), 2363 (s br), 2341 (m br), 2244 (m br), 2161 (w br), 2151 (w br), 2100 (w br), 2041 (w br), 2021 (sh), 1208 (w), 1169 (m), 1152 (m), 1083 (w), 1032 (m), 1017 (m), 965 (sh), 943 (s), 917 (sh), 892 (w), 845 (w), 804 (w), 772 (w), 735 (sh), 721 (s).

Crystallographic Studies.[69] Single crystals of $Cr(B_3H_8)_2$, **2**, grown by sublimation, were mounted on glass fibers with Krytox oil (DuPont) and immediately cooled to −75 °C in a nitrogen gas stream on the diffractometer. Single crystals of $Cr(B_3H_8)_2(Et_2O)_2$, **3**, $Cr(B_3H_8)_2(THF)_2$, **4**, and $Cr(B_3H_8)_2(PMe_3)_2$, **5**, grown from diethyl ether, were treated similarly, except that **4** and **5** were mounted with Paratone-N oil (Exxon). Data for **2**−**5** were collected with an area detector by using the measurement parameters listed in Table 1. The measured intensities were reduced to structure factor amplitudes and their estimated standard deviations by correction for background, Lorentz, and polarization effects. Although corrections for crystal decay were unnecessary, face-indexed (**2**−**5**) absorption corrections were applied. Systematically absent reflections were deleted, and symmetry-equivalent reflections were averaged to yield the sets of unique data. All structures were solved using direct methods (SHELXTL). The correct positions for all non-hydrogen atoms were deduced from E maps. Subsequent least-squares refinements and difference Fourier calculations revealed the positions of the hydrogen atoms attached to boron for all structures. The analytical approximations to the scattering factors were used, and all structure factors were corrected for both real and imaginary components of anomalous dispersion. Final refinement parameters for **2**−**5** are given in Table 1. Subsequent discussions for **2**−**5** will be divided into individual paragraphs.

2: The triclinic lattice suggested the space groups $P1$ and $P\bar{1}$, and the latter was found to be correct. All 925 unique data were used in the least-squares refinement. The quantity refined in the least-squares program was $\sum w(F_o^2 - F_c^2)^2$, where $w = \{[\sigma(F_o^2)]^2 + (0.0560P)^2\}^{-1}$ and $P = (F_o^2 + 2F_c^2)/3$. In the final cycle of least squares, independent anisotropic displacement factors were refined for the non-hydrogen atoms. The hydrogen atoms were located in the difference maps, and their positions were refined with independent isotropic displacement parameters. Successful convergence was indicated by the maximum shift/error of 0.000 for the last cycle. The largest peak in the Fourier difference map (0.42 e Å^{-3}) was located 0.87 Å from the chromium atom. A final analysis of variance between observed and calculated structure factors showed no apparent errors.

3: Systematic absences for $0k0$ ($k \neq 2n$) and $h0l$ ($l \neq 2n$) were only consistent with space group $P2_1/c$. The crystal was twinned, and nine reflections that evidently were affected by the twinning were deleted. The remaining 2157 unique data were used in the least-squares refinement. The quantity refined in the least-squares program was $\sum w(F_o^2 - F_c^2)^2$, where $w = \{[\sigma(F_o^2)]^2 + (0.0306P)^2\}^{-1}$ and $P = (F_o^2 + 2F_c^2)/3$. In the final cycle of least squares, independent anisotropic displacement factors were refined for the non-hydrogen atoms. The hydrogen atoms were located in the difference maps, and their positions were refined with independent isotropic displacement parameters. Successful convergence was indicated by the maximum shift/error of 0.000 for the last cycle. The largest peak in the final Fourier difference map (0.33 e Å^{-3}) was located 1.07 Å from the chromium atom. A final analysis of variance between observed and calculated structure factors showed no apparent errors.

4: Systematic absences for $0k0$ ($k \neq 2n$) and $h0l$ ($h + l \neq 2n$) were only consistent with space group $P2_1/n$. All 2059 unique data were used in the least-squares refinement. Subsequent least-squares refinement and difference Fourier calculations revealed the positions of the boron-bound hydrogen atoms and showed that the β carbon atoms of the THF ligand were disordered over two sites. Site occupancy factors (SOF) summing to 1 were assigned to these sites and the SOF for the major site refined to 0.56(2). The quantity refined in the least-squares program was $\sum w(F_o^2 - F_c^2)^2$, where $w = \{[\sigma(F_o^2)]^2 + (0.0629P)^2\}^{-1}$ and $P = (F_o^2 + 2F_c^2)/3$. In the final cycle of least squares, independent anisotropic displacement parameters were refined for the non-hydrogen atoms. The boron-bound hydrogen atoms were located in the difference maps, and their positions were refined with independent isotropic displacement parameters. The THF-bound hydrogen atoms were fixed in "idealized" positions with C−H = 0.99 Å, and their displacement parameters were set equal to 1.2 times U_{eq} for the attached carbon. An isotropic extinction parameter was refined to a final value of $x = 0.000032(5)$, where F_c is multiplied by the factor $k[1 + F_c^2 x\lambda^3/\sin 2\theta]^{-1/4}$, with k being the overall scale factor. Successful convergence was indicated by the maximum shift/error of 0.000 for the last cycle. The largest peak in the final Fourier difference map (0.37 e Å^{-3}) was located 0.42 Å from the chromium atom. A final analysis of variance between observed and calculated structure factors showed no apparent errors.

5: Systematic absences for $0kl$ ($k \neq 2n$), $h0l$ ($l \neq 2n$), and $hk0$ ($h \neq 2n$) were only consistent with space group *Pbca*. All 4349 unique data were used in the least-squares refinement. The quantity minimized by the least-squares program was $\sum w(F_o^2 - F_c^2)^2$, where $w = \{[\sigma(F_o^2)]^2 + (0.0408P)^2\}^{-1}$ and $P = (F_o^2 + 2F_c^2)/3$. The locations of the hydrogen atoms attached to boron were refined without constraints; these hydrogen atom were each given independent isotropic displacement parameters. Hydrogen atoms attached to carbon were placed in idealized tetrahedral locations with C−H = 0.98 Å, and their locations were optimized by rotation about the P−C bonds; their displacement parameters were set equal to 1.5 times U_{eq} for the attached carbon atom. Successful convergence was indicated by the maximum shift/error of 0.000 for the last cycle. The largest peak in the final Fourier difference map (0.36 e Å^{-3}) was located 0.86 Å from the chromium atom. A final analysis of variance between observed and calculated structure factors showed no apparent errors.

Acknowledgment. We thank the National Science Foundation for support of this research under Grant Numbers DMR03-54060 and DMR04-20768 and Scott R. Wilson and Teresa Prussak-Wieckowska for collecting the X-ray crystallographic data.

Supporting Information Available: X-ray crystallographic files in CIF format for **2**−**5**. This material is available free of charge via the Internet at http://pubs.acs.org.

IC0621300

(69) For a description of the crystallographic programs and procedures used, see: Brumaghim, J. L.; Priepot, J. G.; Girolami, G. S. *Organometallics* **1999**, *18*, 3139−2144.